Neuron, Vol. 25, 239–252, January, 2000, Copyright ©2000 by Cell Press

Mice Lacking α-Synuclein Display Functional Deficits in the Nigrostriatal Dopamine System

Asa Abeliovich,[1,7] Yvonne Schmitz,[4,7] Isabel Fariñas,[2,7] Derek Choi-Lundberg,[3,7] Wei-Hsien Ho,[3] Pablo E. Castillo,[5] Natasha Shinsky,[3] Jose Manuel Garcia Verdugo,[2] Mark Armanini,[3] Anne Ryan,[3] Mary Hynes,[3] Heidi Phillips,[3] David Sulzer,[4] and Arnon Rosenthal[3,6]

[1]Department of Neurology
University of California, San Francisco
San Francisco, California 94143
[2]Department Biología Celular
Universidad de Valencia
46100 Burjasot
Spain
[3]Department of Neuroscience
Genentech
South San Francisco, California 94080
[4]Departments of Neurology and Psychiatry
Columbia University
New York State Psychiatric Institute
Department of Neuroscience
New York, New York 10032
[5]Nancy Friend Pritzker Laboratory
Departments of Psychiatry
and Behavioral Sciences
Stanford University School of Medicine
Palo Alto, California 94304

Summary

α-Synuclein (α-Syn) is a 14 kDa protein of unknown function that has been implicated in the pathophysiology of Parkinson's disease (PD). Here, we show that α-*Syn*$^{-/-}$ mice are viable and fertile, exhibit intact brain architecture, and possess a normal complement of dopaminergic cell bodies, fibers, and synapses. Nigrostriatal terminals of α-*Syn*$^{-/-}$ mice display a standard pattern of dopamine (DA) discharge and reuptake in response to simple electrical stimulation. However, they exhibit an increased release with paired stimuli that can be mimicked by elevated Ca^{2+}. Concurrent with the altered DA release, α-*Syn*$^{-/-}$ mice display a reduction in striatal DA and an attenuation of DA-dependent locomotor response to amphetamine. These findings support the hypothesis that α-Syn is an essential presynaptic, activity-dependent negative regulator of DA neurotransmission.

Introduction

α-Synuclein (α-Syn) was initially isolated from cholinergic nerve terminals of the Torpedo ray electric organ (Maroteaux et al., 1988). Mammalian α-Syn was subsequently found to be prominently expressed in regions of the adult central nervous system (CNS) that display synaptic plasticity, including the cerebral cortex, hippocampus, amygdala, and olfactory bulb (Maroteaux and Scheller, 1991; Iwai et al., 1995). The zebra finch α-Syn homolog synelfin has also been implicated in synaptic plasticity since it is expressed in the lateral magnocellular nucleus, a brain area that participates in seasonal song learning (George et al., 1995).

α-Syn belongs to a family of structurally related proteins that are prominently expressed in the CNS and includes β-Syn and γ-Syn (Jakes et al., 1994; Buchman et al., 1998; Lavedan, 1998). The subcellular localization of the synucleins has not been established definitively, and suggested sites of action include the presynaptic terminal, the nuclear envelope, and the cytoplasm (Maroteaux and Scheller, 1991; Iwai et al., 1995; Lavedan, 1998). The synucleins all possess a highly conserved amino-terminal repeat domain that may mediate both lipid binding and dimerization (Jensen et al., 1997). In addition, they share a common "natively unfolded" tertiary structure that has been implicated in protein–protein interactions (Weinreb et al., 1996; Davidson et al., 1998). Reported binding targets for α-Syn and β-Syn include phospholipase D2 (PLD2; Jenco et al., 1998), an enzyme that catalyzes the production of the intracellular mediators phosphatidic acid (PA) and diacylglycerol (DAG) (Klein et al., 1995; Jenco et al., 1998), and protein kinase C (Ostrerova et al., 1999).

Although its physiological activity remains unclear, α-Syn has been implicated in the etiology of two common neurodegenerative disorders, Alzheimer's disease (AD) and Parkinson's disease (PD). The pathological hallmark of AD involves widespread depositions (termed amyloid plaques) of a 42 amino acid β-amyloid peptide (Aβ) concomitant with the degeneration of hippocampal and cortical neurons. The cause of Aβ depositions is not fully understood. However, a fragment of α-Syn termed the nonamyloid component (NAC; Ueda et al., 1993) was found to be an integral constituent of these plaques in the AD brain. Moreover, NAC binds to β-amyloid peptide in vitro and facilitates its aggregation (Jensen et al., 1995, 1997; Paik et al., 1998), raising the possibility that NAC facilitates plaque formation and the progression of AD.

PD brain pathology is typified by the presence of abnormal protein aggregates, termed Lewy bodies, and selective loss of dopamine (DA) neurons. α-Syn appears to be the major protein component of these intracytoplasmic deposits in sporadic and familial forms of the disease (Mezey et al., 1998; Spillantini et al., 1998). Direct evidence for the involvement of α-Syn in PD was provided by genetic studies of patients with rare, dominantly inherited variants of this disorder. Two independent pathological mutations have been described, a change from alanine to threonine at position 53 in Italian-American and Greek families (Polymeropoulos et al., 1997) and a change from alanine to proline at position 30 in a family of German origin (Krüger et al., 1998). These mutant proteins display a propensity to form Lewy body–like fibrils in vitro (Conway et al., 1998).

[6]To whom correspondence should be addressed (e-mail: ar@ruby.gene.com).
[7]These authors contributed equally to this work.

Given the evidence that α-Syn plays a role in PD and AD, we undertook to determine its normal function by the analysis of α-*Syn*-deficient mice. α-*Syn*$^{-/-}$ mice are viable; possess a wild-type (wt) complement of DA neurons, fibers and synaptic terminals; and reveal a normal time course of DA release and reuptake in response to a single electrical pulse stimulus of nigrostriatal terminals. Surprisingly, the mutant mice exhibit accelerated recovery of DA release when presented with multiple stimuli. Similar accelerated recovery is observed in wt animals in the presence of increased extracellular Ca^{2+}. The α-*Syn*$^{-/-}$ mice also suffer a reduction in total striatal DA and display an attenuated locomotor response to amphetamine. These findings support the idea that α-Syn is an essential, activity-dependent negative regulator of DA neurotransmission that may modulate a process requiring Ca^{2+}.

Results

Generation of α-*Syn*$^{-/-}$ Mice

An α-*Syn* gene-targeting construct was generated in which the first two exons, encoding amino acids 1–41 and upstream untranslated sequences, were deleted (Figure 1A). This targeting construct was electroporated into embryonic stem (ES) cells, and three independent clones in which α-*Syn* had been disrupted by homologous recombination were injected into blastocysts to produce α-*Syn*$^{-/-}$ mice (Figures 1B and 1C). The resulting heterozygous (α-*Syn*$^{+/-}$) and homozygous (α-*Syn*$^{-/-}$) mice were viable, normal in size, and fertile and did not display any gross anatomical abnormalities (data not shown). To determine whether the α-*Syn* gene had indeed been inactivated, expression of α-*Syn* mRNA was analyzed by RT-PCR using primers specific for either the deleted 5′ terminus (encoding amino acids 1–92) or the remaining 3′ sequences (encoding amino acids 76–136) of the gene. No transcripts derived either from the 5′ or 3′ regions of α-*Syn* were detected in the brains of the mutant mice (Figure 1D), confirming that the α-*Syn* gene is no longer functional. Western blot analysis of brain homogenates with an antibody specific to the carboxyl terminus of α-Syn further demonstrated the absence of α-Syn protein in these mice (Figure 1E). In contrast, no changes in the levels of β-*Syn* and γ-*Syn* transcripts or protein were detected (Figures 1D and 1E).

In situ hybridization analyses further revealed prominent expression α-*Syn* in the cerebral cortex, hippocampus, striatum, and ventral midbrain of wt mice (Figure 2A). In contrast, β-*Syn* expression appeared to be relatively widespread in the adult CNS (Figure 2B), whereas γ-*Syn* was principally restricted to the DA neurons of the substantia nigra (SN) and ventral tegmental area (VTA; Figure 2C; Lavedan, 1998). α-*Syn* transcripts were absent from the α-*Syn*$^{-/-}$ mice (Figure 2A), whereas the expression patterns for β-*Syn* and γ-*Syn* mRNA appeared normal (Figures 2B and 2C), indicating that the absence of α-Syn had not been compensated for by changes in the tissue distribution or levels of other synuclein family members. Antibody staining for α-Syn protein in the striatum of wt animals reveals a characteristic punctate distribution, consistent with the accumulation of this protein in axons (but not cell bodies; Figure 2D). This protein was completely absent from the striatum of the α-*Syn*$^{-/-}$ mice (Figure 2D). In contrast, axons in the striatum were immunopositive for β-Syn both in wt and α-*Syn*$^{-/-}$ mice (Figure 4C).

α-Syn Is Not Essential for Neuronal Development or for the Formation of Presynaptic Terminals

Given the finding that human α-*Syn* mutations lead to the degeneration of DA neurons in the ventral midbrain, we examined the status of this neuronal population in the α-*Syn*$^{-/-}$ mice. Surprisingly, 3- to 6-week-old α-*Syn*$^{-/-}$ animals possess a typical complement of tyrosine hydroxylase positive (TH+) midbrain DA neurons in the SN (midbrain DA neuronal counts from alternating sections through the SN: wt, 3273 ± 15, $n = 3$; α-*Syn*$^{-/-}$, 3396 ± 52, $n = 3$; Figure 3A). Moreover, the DA neurons appear morphologically indistinguishable from wt (Figure 3B), and the density of DA projections to the striatum (the nigrostriatal pathway; Figure 3C) is normal. In addition, neurons and support cells in the striatum itself appear unaltered, as determined by the number and morphology of cells positive for neuropeptide Y, somatostatin, parvalbumin, calretinin, TrkA, γ-aminobutyric acid (GABA), and glial fibrillary acid protein (Figure 3D; data not shown). The general striatal matrix architecture, as indicated by calbindin staining, is also preserved in mutant mice. Finally, the α-*Syn*$^{-/-}$ mice do not display any gross morphological deficits in midbrain, striatum, cerebellum, basal forebrain, hippocampus, or cerebral cortex, as determined by toluidine blue staining (data not shown), indicating that α-Syn is not required for neuronal development and differentiation.

As α-Syn has been hypothesized to function in vesicular neurotransmitter release (Clayton and George, 1998), we next investigated whether its absence would alter the expression and distribution of well-characterized synaptic vesicle proteins (Südhof, 1995). To this aim, brain sections from α-*Syn*$^{-/-}$ and wt mice were immunostained with antibodies specific for the proteins Rab3a, synapsin-I, synaptophysin, and β-Syn. The distribution of these proteins appears to be unaltered in the mutant mice, suggesting that the loss of α-Syn does not lead to gross alterations in the protein composition of synaptic terminals (Figures 4A–4C; data not shown). We further employed electron microscopy to determine whether the absence of α-Syn leads to changes in synaptic density or structural aberrations in synaptic terminals. The synaptic density in the striatum of the *Syn*$^{-/-}$ mice was indistinguishable from that of wt littermates (wt, 18.7 ± 0.4 synapses/100 μm^2, $n = 3$; *Syn*$^{-/-}$, 19.2 ± 0.9 synapses/100 μm^2, $n = 3$). Furthermore, presynaptic dense projections, postsynaptic densities, and synaptic vesicles all appear normal in morphology and distribution throughout the striatum and hippocampus of the α-*Syn*$^{-/-}$ mice, when compared with wt siblings (Figure 4D; data not shown). Thus, α-Syn may not be an essential structural component of presynaptic terminals.

α-Syn Is Not Essential for Release and Reuptake at Dopaminergic Terminals

As α-Syn is prominently expressed at the nerve terminals of nigral DA neurons and, when mutated, can cause

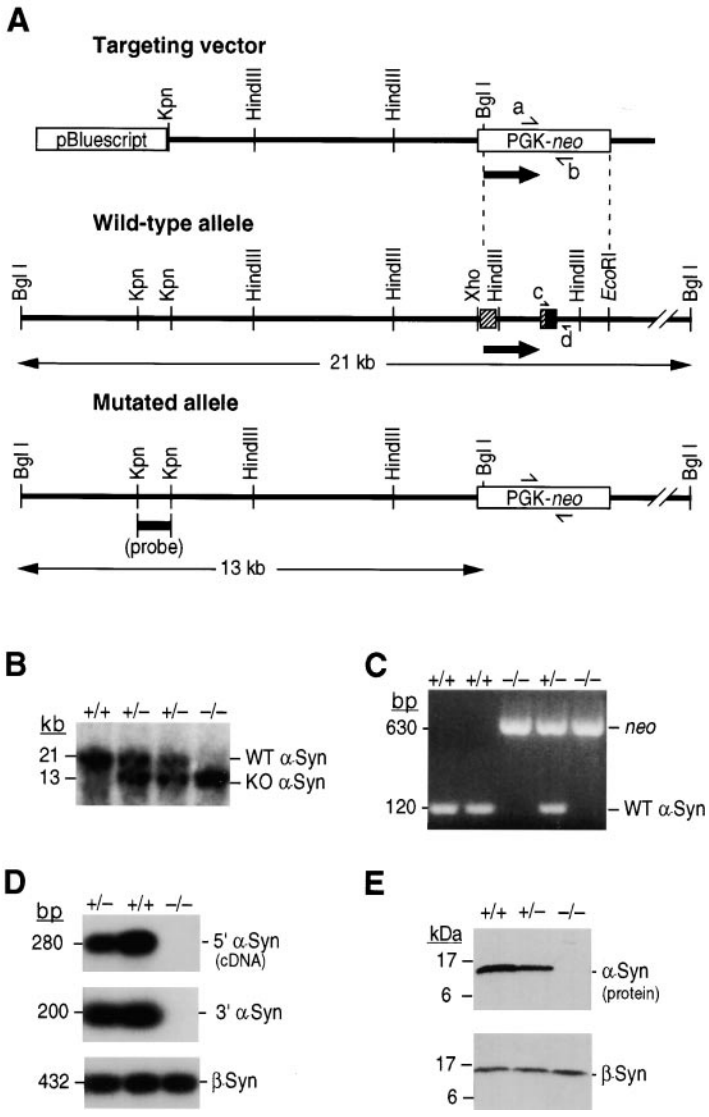

Figure 1. Generation of α-*Syn*$^{-/-}$ Mice

(A) The α-*Syn* targeting vector, wt allele, and mutated allele. The first two exons, encoding amino acids 1–41, are missing from the mutated allele. The location of the probe used in Southern blots is indicated (probe); the neomycin resistance gene, driven by the phosphoglycerate-1 promoter, is marked (*PGK-neo*); the striped and solid boxes represent noncoding and coding sequences of the first two exons, respectively. The directions of gene transcription for *PGK-neo* and α-*Syn* are indicated by horizontal solid arrows. Primers ("a–d") were used for PCR amplification in (C).

(B and C) Genotype analyses of tail DNA from wt (+/+), heterozygous mutant (+/−), and homozygous mutant (−/−) mice by Southern blotting (B) and by PCR amplification (C).

(D) RT-PCR analyses of cerebral cortex RNA with primers specific for α-*Syn* 5′ sequences that cover the disrupted exons, α-*Syn* 3′ sequences, or β-*Syn*.

(E) Western blot analyses of α-Syn and β-Syn protein.

their degeneration, we sought to examine whether it might regulate synaptic function in the nigrostriatal pathway. Striatal slice preparations containing presynaptic DA terminals were stimulated by a single electrical pulse (400 μA, 1 ms) or a train of 10 such pulses at 50 ms intervals (20 Hz), which approximates the observed "burst firing" pattern of nigral DA neurons in vivo (Grace and Bunney, 1984). Following stimulation, the concentration and kinetics of DA release were measured using fast-scan cyclic voltammetry (CV; Figure 5A; Wightman and Zimmerman, 1990; Kennedy et al., 1992). In response to electrical stimulation, a rapid rise in the level of extracellular DA is observed (Figure 5B), corresponding to Ca^{2+}-dependent neurotransmitter release from small synaptic vesicles (Wightman and Zimmerman, 1990), which is abolished in the presence of 200 μM cadmium (data not shown). The peak DA level is a function of competing mechanisms of synaptic release and reuptake, whereas the time course of the subsequent DA decrement reflects the rates of DA reuptake and diffusion.

The time course of measured extracellular DA, in response to either a single electrical stimulus or a train of stimuli, appeared normal in α-*Syn*$^{-/-}$ mice, indicating that DA reuptake and diffusion are unaltered (data not shown). Similarly, the peak concentration of extracellular DA, in response to either a single electrical pulse or a train of pulses, did not differ significantly between slice preparations from wt and *Syn*$^{-/-}$ mice ($p > 0.05$ for each, two-sample Student's t test; Figure 5C). Taken together, these findings indicate that α-Syn is not involved in the control of DA release in response to simple single or train stimuli.

α-Syn Modulates Paired Stimulus Depression of DA Release

Dynamic changes in DA release are thought to underlie the physiological functions of DA pathways, such as the learning and execution of motor tasks and the recognition of novelty and reward (Rebec et al., 1997). For instance, stimulation-dependent DA release is depressed in the nucleus accumbens during the establishment of

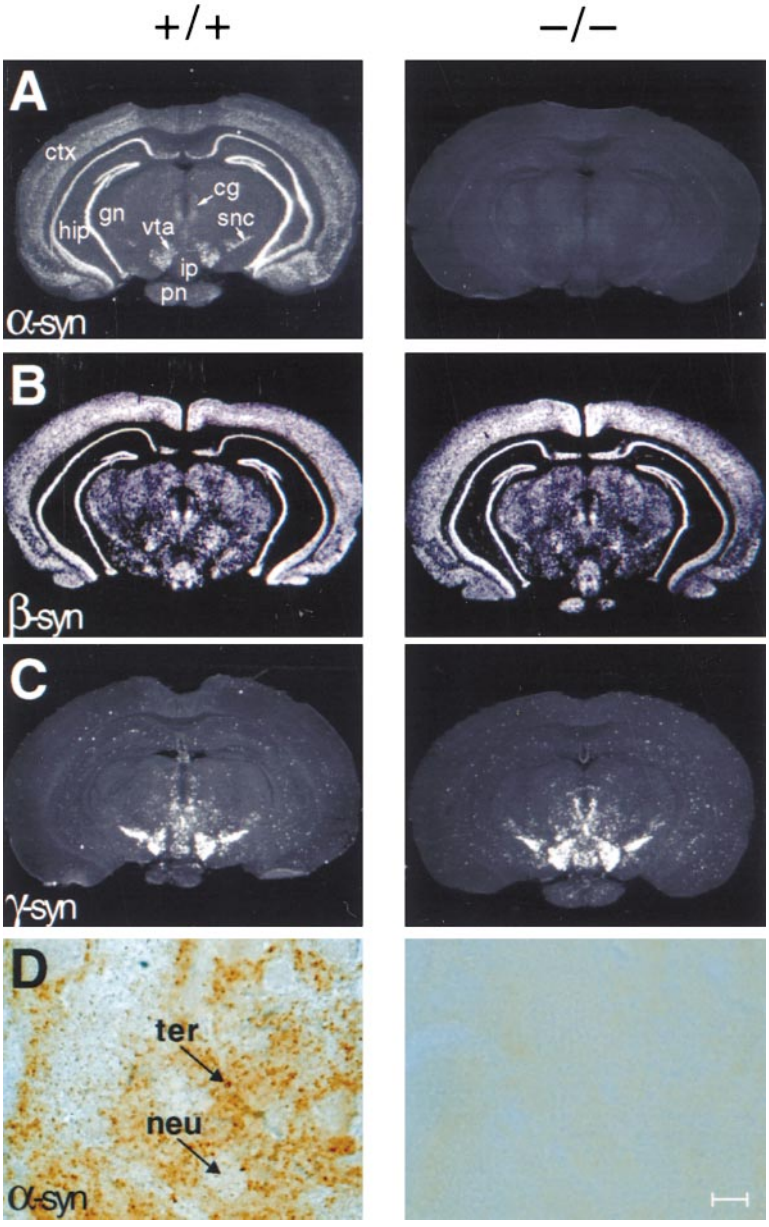

Figure 2. Expression of the Synuclein Family in the CNS

(A–C) Coronal brain sections from wt and α-*Syn*$^{-/-}$ mice were analyzed by in situ hybridization with antisense RNA probes for α-*Syn* (A), β-*Syn* (B), and γ-*Syn* (C). In wt mice, high levels of α-*Syn* expression were observed in the cerebral cortex (ctx), hippocampus (hip), substantia nigra pars compacta (snc), and ventral tegmental area (vta). α-*Syn* expression was not detected in homozygous mutants. β-*Syn* expression was widespread (see text) in both genotypes. γ-*Syn* expression appeared most prominent in the VTA and SNC. (D) Immunohistochemical analysis of α-Syn protein in the striatum.

Abbreviations: gn, geniculate body; cg, central gray; pn, pontine nuclei; ip, interpeduncular nucleus; ter, presynaptic terminal; and neu, neuron. Scale bar, 1 mm (A–C) and 37 μM (D).

intracranial self-stimulating behavior, a model of learning and reward (Garris et al., 1999). Consistent with the nature of DA neurotransmission in vivo, DA release from striatal slice preparations, as evoked by pairs of electrical stimuli, exhibits depression and recovery that are dependent in part on DA autoreceptors (Starke et al., 1989; Kennedy et al., 1992; Garris et al., 1999). We sought to examine whether α-Syn plays a role in activity-induced modulation of synaptic DA release.

Striatal brain slices (containing DA terminals from the nigrostriatal pathway) were electrically stimulated with paired pulses (1 ms, 400 μA) at interpulse intervals ranging from 2.5 to 60 s (Figure 5D), and peak extracellular DA levels in response to each stimulus were measured using CV. In slices from wt mice, peak DA levels following the second stimulus were reduced as compared with the peak levels following the first stimulus for interpulse intervals of <60 s (Figures 5D and 5E). We designated this phenomenon paired stimulus depression (PSD). In contrast, when striatal slices from α-*Syn*$^{-/-}$ mice were exposed to the same paired electrical stimuli, the recovery of DA release was significantly faster ($p < 0.01$ for 5, 10, 20, and 30 s time intervals, two-way ANOVA for repeated measures with subsequent Newman-Keuls test; Figures 5D and 5E). As reported for rat nigrostriatal terminals (Kennedy et al., 1992), the time course for synaptic recovery is well described by a double exponential function (Figure 5E). In wt animals, the time constants for the slow component, τ_s, and the fast component, τ_f, were 24 s and 6 s, respectively ($n = 20$ slices from 12 animals). In contrast, the time constants for recovery of peak DA levels at α-*Syn*$^{-/-}$ terminals were 16 s for τ_s and 5 s for τ_f ($n = 24$ slices from 14 animals).

Unlike their wt siblings, all the of α-*Syn*$^{-/-}$ 129SV/j ×

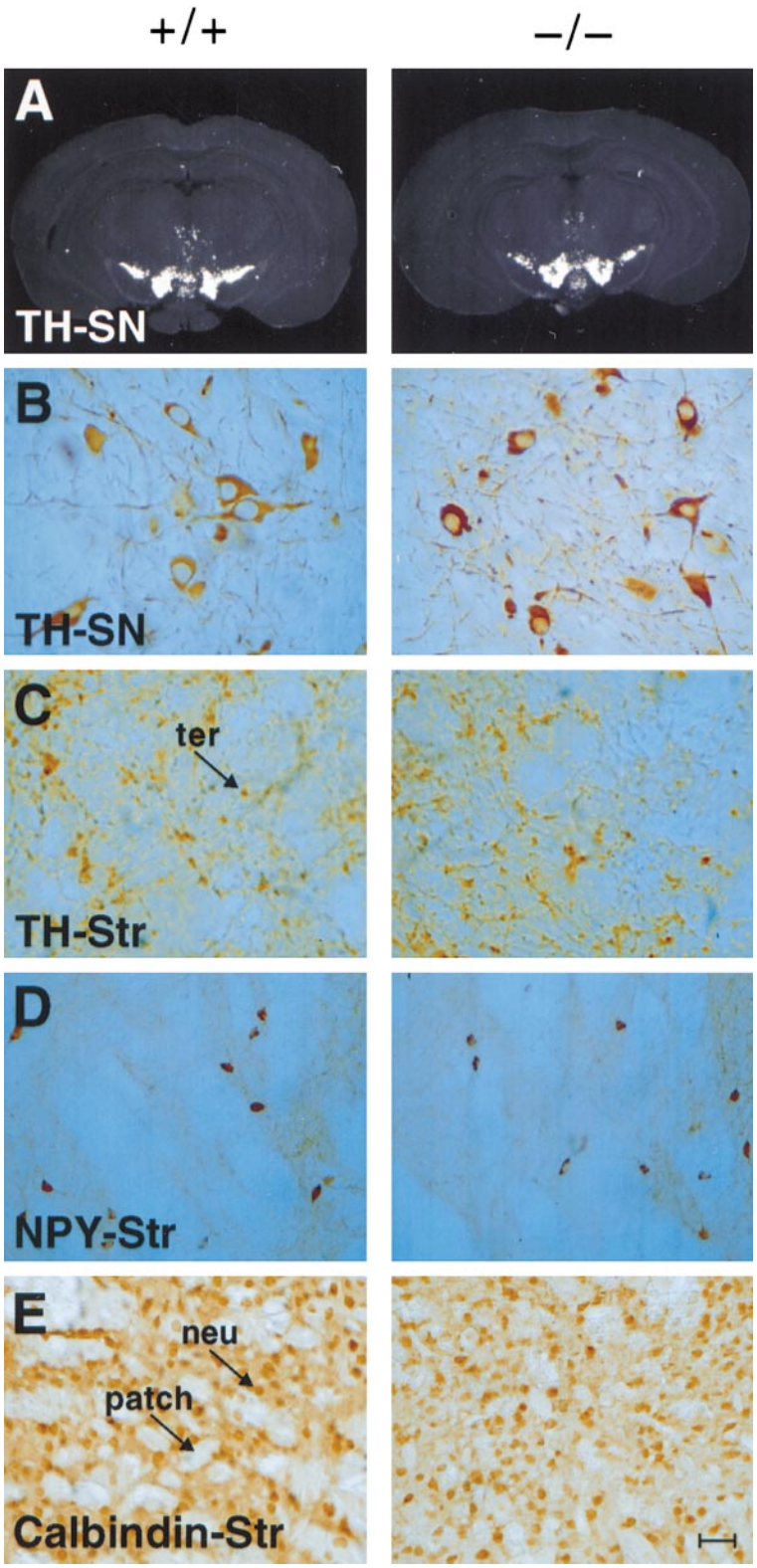

Figure 3. Morphology of the Nigrostriatal Pathway in wt and α-*Syn*$^{-/-}$ Mice

(A) In situ hybridization of coronal brain sections with a probe for *TH*, the rate-limiting enzyme in DA synthesis.

(B–E) Staining of coronal sections through the SN (B) and the striatum (C–E) with antibodies for TH (B and C), neuropeptide Y (D), or calbindin (E). No deficits or abnormalities in neuronal number, morphology, or innervation pattern are observed in the α-*Syn*$^{-/-}$ mice.

Abbreviations: patch, striatal matrix patch, and neu, neuron. Scale bar, 1 mm (A); 104 μm (B); 44 μm (C); 147 μm (D); and 139 μm (E).

C57/BL6 F2 mice are homozygous for an α-*Syn* locus that is derived from the 129SV/j origin. Thus, it remained possible that the observed deficits are due to a gene that is linked to the 129SV/j-derived α-*Syn* and not to the α-Syn deficiency. To exclude this possibility, we have identified and analyzed 129SV/j × C57/BL6 F2 mice that are homozygous for the wt 129SV/j-derived α-*Syn* locus (see Experimental Procedures). These mice (n = 5) displayed PSD with a time course identical to that observed for the wt littermates of the α-*Syn*$^{-/-}$. Taken

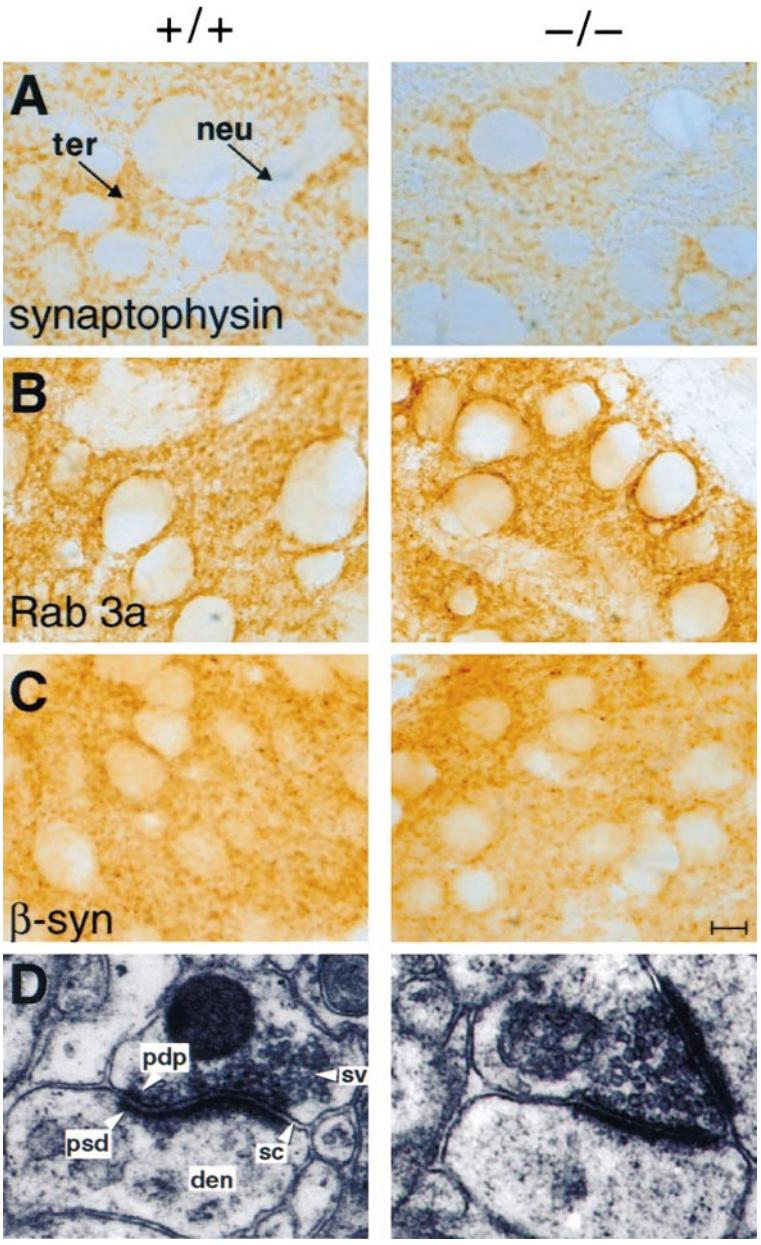

Figure 4. Expression of Presynaptic Terminal Proteins in wt and α-*Syn*$^{-/-}$ Mice

(A–C) Coronal slices of the striatum were stained for the vesicular release proteins synaptophysin (A) and Rab3a (B), as well as for β-Syn (C). These proteins are all expressed at vesicular release sites, and their expression appears normal in the α-*Syn*$^{-/-}$ mice.

(D) Electron micrographs of synaptic terminals in the striatum. The morphology and distribution of synaptic boutons and neurotransmitter vesicles appeared unaltered in α-*Syn*$^{-/-}$ mice.

Abbreviations: psd, postsynaptic density; sv, synaptic vesicles; den, dendrite; sc, synaptic cleft; and pdp, presynaptic dense projections. Scale bar, 29 μm (A); 22 μm (B); 26 μm (C); and 0.2 μm (D).

together, these findings strongly support the idea that α-Syn deficiency accelerates the recovery of DA release following an initial stimulus and suggest an inhibitory role for this protein in the activity-dependent modulation of DA neurotransmission.

To further define the scope of the alteration in DA neurotransmission, we next investigated DA release in response to other stimulation patterns. Specifically, we examined the recovery of DA release for pairs of burst-like stimuli since the observed firing frequency of nigral DA neurons in vivo displays both single action potential spikes and bursts of firing (consisting of three to ten spikes at 10–20 Hz (Grace and Bunney, 1984). Striatal slice preparations were presented with pairs of 10 pulse, 20 Hz stimulation trains at interburst intervals of 2.5–60 s (Figure 6A), and the peak level of extracellular DA that was released with each train was measured. This peak represents multiple, temporally overlapping DA release events (see Experimental Procedures). As was the case with paired single stimuli, the initial train stimulus led to inhibition of peak DA release to the second train stimulus (Figure 6B). However, in wt animals, the recovery of the peak DA response following train stimulation ($n = 11$ slices from 9 animals) was considerably faster than the recovery following a single pulse ($p < 0.01$ for 2.5, 5, 10, 20, and 30 s time intervals, two-way ANOVA for repeated measures with subsequent Newman-Keuls test; Figure 6B). In contrast, in striatal preparations from α-*Syn*$^{-/-}$ mice, the time course of recovery from train stimulation was only mildly hastened in comparison with single pulse stimulation ($p < 0.01$ for the 5 s interval, two-way ANOVA for repeated measures with subsequent Newman-Keuls test; $n = 10$ slices from 7 animals; Figures 6C and 6E). Furthermore, the recovery from train

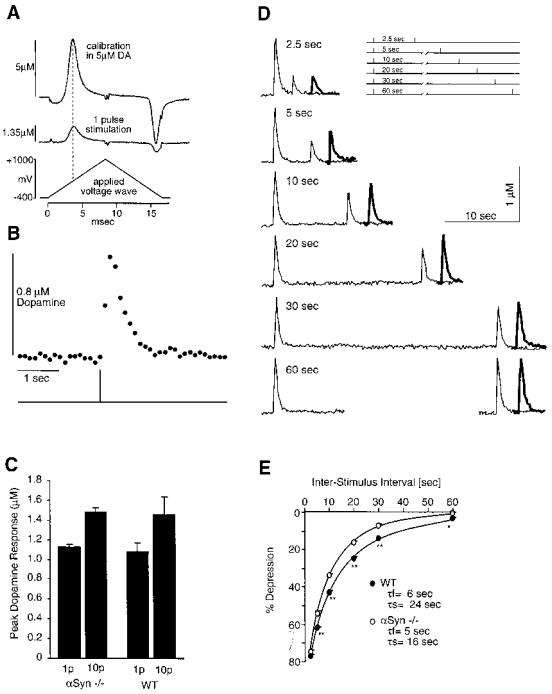

Figure 5. α-*Syn*$^{-/-}$ Mice Exhibit Altered PSD of DA Release

Electrically evoked DA release in striatal slice preparations was measured using carbon-fiber electrodes and fast-scan CV.

(A) Background-subtracted voltammograms depicting measured DA concentration following exposure to 5 μM DA and following 1 pulse stimulation of a striatal slice. DA is identified by virtue of the characteristic oxidation (dashed line) and reduction currents in response to applied voltage wave.

(B) A representative time course of measured DA concentration (scan at 10 Hz) in response to a single electrical pulse (400 μA, 1 ms; schematic at bottom); a rapid rise in DA is observed, followed by a gradual decline.

(C) The peak DA response to either a single pulse (wt, n = 12 slices; α-*Syn*$^{-/-}$, n = 14 slices) or a train stimulus (10 pulses delivered at 20 Hz; wt, n = 6; α-*Syn*$^{-/-}$, n = 10) did not differ significantly between genotypes. In response to a train of 10 pulses at 20 Hz, the measured DA peak represented multiple, temporally overlapping DA release events, and therefore, the response to such train stimulation was significantly greater than to single pulses, regardless of the genotype.

(D) Paired pulse depression is altered in α-*Syn*$^{-/-}$ slices. Paired electrical stimuli were applied at variable interpulse intervals (inset) to slice preparations from wt and α-*Syn*$^{-/-}$ mice. Representative recording traces from wt (thin trace) and from α-*Syn*$^{-/-}$ mutant slices (bold trace; offset for presentation, normalized in amplitude to the first peak of the wt recordings) are shown. Synaptic release recovered significantly faster in α-*Syn*$^{-/-}$ slices than in wt slices.

(E) Averaged time courses for recovery of the peak DA response are presented as the percent depression of the second stimulus response relative to the first (100 × [1 − s peak amplitude/first peak amplitude]) in wt (n = 20 slices from 16 animals) and α-*Syn*$^{-/-}$ (n = 24 slices from 14 animals) slices. Data were fitted by double exponential functions (solid lines) of the form [50 × exp(−k1 × x)] + [50 × exp (−k2 × x)]; τ_s, slow component time constant; τ_f, fast component time constant. Error bars represent standard error of the mean.

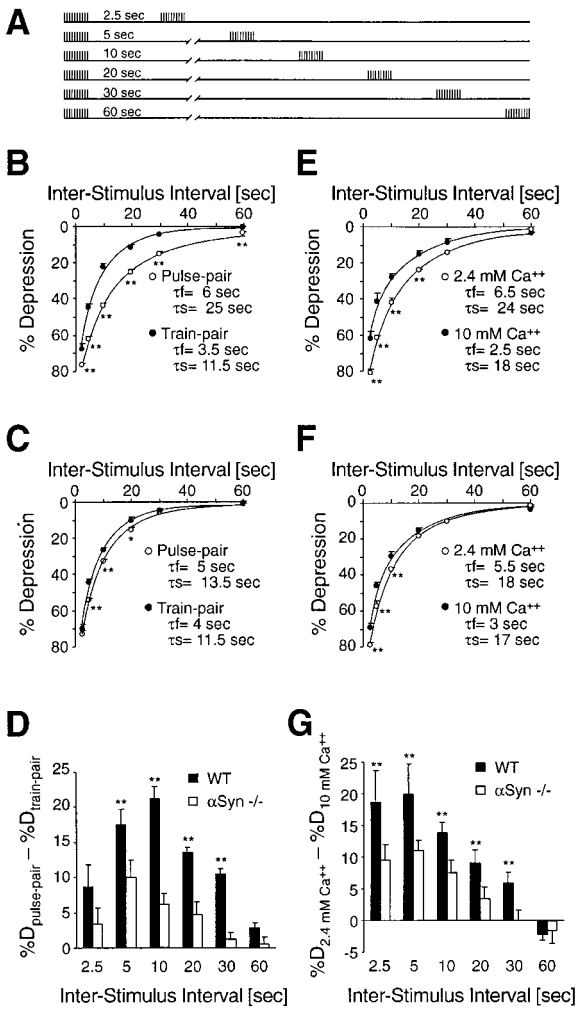

Figure 6. The Alteration in DA Release in the α-*Syn*$^{-/-}$ Mice Is Dependent on the Mode of Stimulation and the Bath Divalent Ion Composition

(A) Striatal slices were presented with a pulse pair, as depicted schematically in Figure 5D (inset), or with pairs of 10 pulse, 20 Hz stimulation trains at variable interstimulus intervals, as depicted.

(B and C) DA synapses from wt (B) and α-*Syn*$^{-/-}$ (C) mice differ significantly in their ability to recover from single pulse depression, as in Figure 5E. However, synaptic recovery from a stimulus train is similar in the two genotypes (wt, n = 11 slices from 9 animals; α-*Syn*$^{-/-}$, n = 10 slices from 7 animals).

(D) The nature of the stimulation protocol had a more profound effect on the time course of synaptic recovery in the wt than the mutant mice. This is presented as the difference in percent depression between the two stimulation protocols ($\%D_{\text{pulse-pair}} - \%D_{\text{train-pair}}$).

(E and F) In the presence of increased extracellular Ca^{2+} (10 mM versus 2.4 mM), synaptic recovery from a single pulse stimulus was significantly hastened in slices from wt mice ([E], 4 slices from 3 animals), whereas mutant slices ([F], 10 slices from 5 animals) were less affected. Moreover, the two genotypes did not differ significantly in their recovery from depression in the presence of increased extracellular Ca^{2+}.

(G) The affect of increased extracellular Ca^{2+} on synaptic recovery was more prominent in slices from wt than from α-*Syn*$^{-/-}$ mice. This is presented as the difference in percent depression between the two conditions ($\%D_{2.4\text{ mM } Ca^{2+}} - \%D_{10\text{ mM } Ca^{2+}}$).

stimulation did not differ significantly between the two genotypes (Figures 6B and 6C). Taken together, these findings indicate that α-Syn does not regulate DA neurotransmission in response to pairs of burst-like stimuli.

Given the finding that electrically evoked DA release

is altered in the α-*Syn* mutant mice, we also examined the affect of α-Syn deficiency on amphetamine-stimulated DA release. DA release in response to amphetamines differs considerably from electrically evoked vesicular exocytosis in that it is Ca^{2+} independent and mediated by "reverse transport" of the plasma membrane DA transporter (Sulzer et al., 1995; Fon et al., 1997; Jones et al., 1998). Peak extracellular DA levels evoked by 10 μM amphetamine sulfate appeared normal in α-*Syn*$^{-/-}$ mice (wt, 1.93 ± 0.43 μM, n = 5; α-*Syn*$^{-/-}$, 2.16 ± 0.49 μM, n = 7), indicating that amphetamine-regulated DA release and reuptake do not require the presence of α-Syn.

α-Syn Does Not Change PSD through a D2 Autoreceptor Pathway

The mechanism by which recent past stimuli depress subsequent DA neurotransmission is not well understood. However, DA D2 autoreceptors, which are present on the presynaptic membrane, have been implicated. Activation of DA D2 autoreceptors can lead to a decrease in subsequent DA release, whereas D2 antagonists appear to accelerate the time course of synaptic recovery (Kennedy et al., 1992). To investigate whether the observed differences in PSD between wt and α-*Syn*$^{-/-}$ mice might be due to a difference in autoreceptor activity, we repeated the above experiments in the presence of the D2 receptor antagonist sulpiride. The PSD recovery time and magnitude of peak DA release following a single stimulus were unaltered by sulpiride, regardless of the genotype (n = 4 for both genotypes), indicating that autoreceptor activation does not modulate PSD for single stimuli. In contrast, as previously noted (Kennedy et al., 1992), sulpiride appeared to potentiate the peak level of DA release in response to a single 10 pulse stimulus train (~130%; data not shown). Moreover, in both genotypes, sulpiride significantly accelerated the time course for PSD recovery of peak DA release following train stimulation (wt with sulpiride, τ_s = 5.5 s; wt without sulpiride, τ_s = 12.5 s, n = 3; α-*Syn*$^{-/-}$ with sulpiride, τ_s = 4.5 s; α-*Syn*$^{-/-}$ without sulpiride, τ_s = 11 s, n = 4). Taken together, these data indicate that recovery from train stimulation, but not from a single stimulus, is attenuated by the DA D2 autoreceptor and that α-Syn inhibits synaptic recovery by a mechanism independent of the D2 autoreceptors.

The Effects of α-Syn Can Be Simulated by Ca^{2+}

Short-term depression (with a decay time constant of 5–30 s) at certain CNS synapses has been interpreted as the depletion of a limited pool of readily releasable synaptic vesicles (RRP; Dittman and Regehr, 1998; Stevens and Wesseling, 1998; Wang and Kaczmarek, 1998; Gomis et al., 1999). According to this model, once the RRP is emptied by an initial stimulus, the response to subsequent stimulation depends on the size and rate of refilling of this pool. Furthermore, refilling of the RRP appears to be accelerated by high-frequency stimulation or increased extracellular Ca^{2+}. Given the similar time course and activity dependence of PSD that we observe, we investigated whether recovery from PSD in striatal slices is Ca^{2+} dependent.

As expected, given the involvement of Ca^{2+} in synaptic vesicle fusion, blockade of Ca^{2+} channels with 200 μM cadmium led to the elimination of DA release in wt striatal slices (data not shown). In addition, DA release following a single stimulation was potentiated (1.7-fold in wt mice, 1.8-fold in the α-*Syn*$^{-/-}$ mutants) when Ca^{2+} levels were raised from 2.4 mM to of 10 mM. More importantly, in slices from wt mice, the recovery from PSD was significantly hastened by higher Ca^{2+} concentrations. Thus, in the presence of 2.4 mM Ca^{2+}, the slow component of the recovery from PSD displayed a time constant of τ_s = 24 s, and the fast component a time constant of τ_f = 6.5 s (n = 4 slices from 3 animals). In contrast, in the presence of 10 mM Ca^{2+}, τ_s was 18 s and τ_f was 2.5 s (Figure 6E). Surprisingly, PSD was less affected by elevated Ca^{2+} in slices from the mutant mice. Thus, α-*Syn*$^{-/-}$ striatal slices displayed a τ_s of 18 s and τ_f of 5.5 s with 2.5 mM Ca^{2+}, and a τ_s of 17 s and τ_f of 3.0 s in the presence of 10 mM Ca^{2+} (n = 10 slices from 5 animals; Figures 6F and 6G). Taken together, these results suggest that α-Syn and extracellular Ca^{2+} regulate PSD recovery by similar mechanisms and are consistent with the notion that PSD is a consequence of the depletion of a RRP of synaptic vesicles.

α-Syn Is Not Essential for Long-Term Potentiation of Glutamatergic Synapses in the Hippocampus

As α-Syn expression is prominent in the adult hippocampus (Figure 2A), we next investigated whether mutant animals display altered synaptic modulation in this region. Tissue slices were prepared from the hippocampus of wt and α-*Syn*$^{-/-}$ mice, and long-term potentiation (LTP) of excitatory synapses in the CA1 region of the hippocampus was elicited by tetanic electrical stimulation at 100 Hz for 1 s, repeated four times every 20 s (Castillo et al., 1997; Schlüter et al., 1999). Robust N-methyl-D-aspartate receptor–dependent LTP was observed in both wt and α-*Syn*$^{-/-}$ mice (Figure 7A). Similarly, the *Syn*$^{-/-}$ excitatory mossy fiber output from the dentate granule cells to the pyramidal cells in the CA3 region of the hippocampus displayed normal mossy fiber LTP (Figure 7A), a presynaptic form of glutamatergic plasticity (Tong et al., 1996). Thus, α-Syn does not appear to be required for these forms of glutamatergic synaptic modulation.

DA Content Is Reduced in Mutant Mice

Given the alteration in DA release, we next examined whether the absence of α-Syn leads to a change in striatal DA content, the bulk of which is stored in synaptic vesicles (Fon et al., 1997; Jones et al., 1998). Quantification by reverse-phase high-pressure liquid chromatography (HPLC) in tissue punch biopsies revealed that DA content was significantly reduced in the striatum of α-*Syn*$^{-/-}$ mice, as compared with wt mice (18% reduction, Student's t test, p = 0.004; Figure 7B). DA content in the ventral midbrain (SN+ VTA) and nucleus accumbens was comparable in the two genotypes (data not shown). Additionally, we measured the striatal content of the major DA metabolite 3,4-dihydroxyphenylacetic acid (DOPAC). The ratio of DOPAC:DA is thought to reflect the relative rate of DA degradation (turnover or utilization; Horger et al., 1998). We found that the absolute concentration of striatal DOPAC was comparable in the two

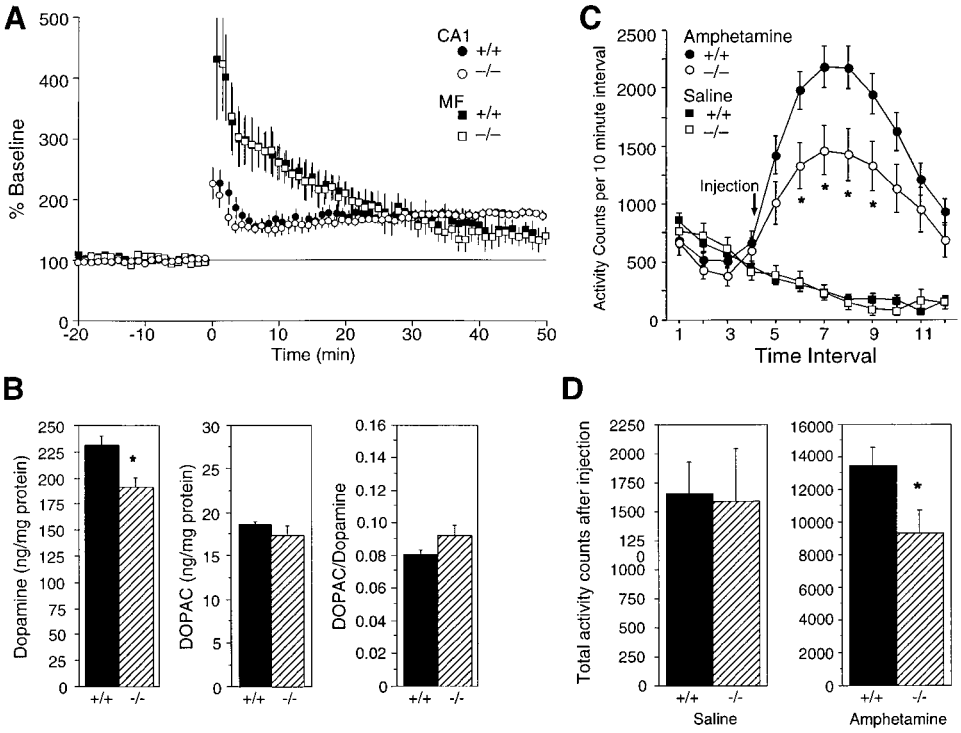

Figure 7. α-*Syn*$^{-/-}$ Mice Display Normal LTP but Reduced Striatal DA Content and Decreased Sensitivity to Amphetamine-Stimulated Locomotion

(A) LTP appears unaltered at the hippocampal mossy fiber–CA3 and Schaffer collateral–CA1 synapses of α-*Syn*$^{-/-}$ mice. Induction of LTP by tetanic stimulation (at Time = 0; see Experimental Procedures) is observed in hippocampal slices from wt (n = 5) and α-*Syn*$^{-/-}$ (n = 5) mice.
(B) Striatal DA and DOPAC contents were measured in brain punch biopsies from wt and α-*Syn*$^{-/-}$ mice. α-*Syn*$^{-/-}$ mice (n = 9) displayed significantly reduced striatal DA content (18%, Student's t test, p = 0.004) in comparison with wt controls (n = 10). Striatal DOPAC content and the DOPAC:DA ratio did not differ significantly among the genotypes.
(C and D) α-*Syn*$^{-/-}$ (n = 12) and wt (n = 19) mice exhibited similar patterns of activity in the context of a novel environment. Mice were placed in a 38 × 45 cm Plexiglas arena, and locomotion was assessed for 2 hr by the number of times photocell beams were crossed per 10 min interval. An intraperitoneal saline injection was given during the fourth interval (arrow, [C]). wt (n = 19) and homozygous mutant (n = 11) mice both demonstrated an increase in locomotion after an intraperitoneal injection of D-amphetamine (4 mg/kg body weight). However, homozygous mutants displayed a significantly attenuated amphetamine response (repeated measures ANOVA: p = 0.016 for genotype).

genotypes (Figure 7B). Furthermore, the DOPAC:DA ratio was not significantly altered in the mutants, although a trend was noted for higher DOPAC:DA ratios in the striatum of α-*Syn*$^{-/-}$ mice (Student's t test, p = 0.12; Figure 7B). These data suggest that the reduced DA content in the α-*Syn*$^{-/-}$ mice results from decreased DA synthesis or storage. The deficit may reflect either a direct effect of α-Syn deficiency or a compensation for the altered dynamic DA release.

α-Syn Deficiency Does Not Alter Locomotor Activity in a Novel Environment

Modulation of DA neurotransmission is thought to underlie the increased locomotor activity observed when an animal is placed in a novel environment (Rebec et al., 1997; Garris et al., 1999). Given the observed changes in DA neurotransmission and DA content, we sought to determine whether α-*Syn*$^{-/-}$ mice might display altered locomotor behavior when placed in new open-field surroundings. Spontaneous locomotor activity was measured over 2 hr by means of a photocell grid counter. wt and α-*Syn*$^{-/-}$ mice did not differ significantly in this task and displayed a similar pattern of habituation to the novel environment over time (n = 19 wt and n = 12 mutant mice; repeated measures ANOVA: p = 0.34 for genotype × time interaction, $p < 0.0001$ for time; Figures 7C and 7D). Thus, α-Syn is not required for the locomotor response to novelty.

Amphetamine-Stimulated Locomotion Is Reduced in the α-*Syn*$^{-/-}$ Mice

Amphetamines can dramatically stimulate locomotor activity by increasing DA release through multiple mechanisms and by inhibiting its reuptake (Seiden et al., 1993; Wise, 1996). Given the altered striatal DA release and DA content in the α-*Syn*$^{-/-}$ mice, we examined whether amphetamine-mediated locomotor behavior may also be modified. Although amphetamine-regulated DA release and reuptake appear intact in brain slices from mutant animals (see above), we anticipated that the α-*Syn*$^{-/-}$ mice may still display deficits in amphetamine-mediated behaviors since such behavior reflects multiple presynaptic and postsynaptic functions.

We investigated the locomotor response of mutant (n = 12) and wt (n = 19) mice to an intraperitoneal injection of D-amphetamine (4 mg/kg). As mentioned,

spontaneous locomotor activity prior to the injection of D-amphetamine did not differ between the genotypes (Figures 7C and 7D). Subsequent to the amphetamine injection, both wt and mutant animals exhibited increased locomotion, indicating that α-Syn is not essential for the basic response to amphetamine. However, α-*Syn*$^{-/-}$ mice displayed a significantly attenuated response to D-amphetamine, as compared with wt mice (repeated measures ANOVA: $p = 0.0158$ for genotype; Figures 7C and 7D). Given the observation that amphetamine-regulated DA release and reuptake appear normal in the mutants, the decreased locomotor response to amphetamines in α-*Syn*$^{-/-}$ mice likely represents a compensatory postsynaptic change secondary to the observed disinhibited vesicular release.

Discussion

Our analysis of α-*Syn*-deficient mice indicated that they are viable, fertile, and do not display any gross pathological abnormalities. The CNS of α-*Syn*$^{-/-}$ mice appears morphologically intact and possesses a wt complement of DA neurons and nerve terminals. Despite the lack of any morphological abnormalities, the α-*Syn*$^{-/-}$ mice suffer significant neurochemical, electrophysiological, and behavioral deficits. They exhibit faster recovery from PSD and display a reduction in total striatal DA levels, as well as an attenuated locomotor response to amphetamine. These findings are most consistent with the idea that α-Syn is an essential, activity-dependent negative regulator of DA neurotransmission.

Regulation of DA Release Is Altered in the Mutant Mice

α-*Syn*$^{-/-}$ mice are defective in a form of synaptic depression normally exhibited at nigrostriatal terminals that we term PSD. Specifically, we find that the recovery of peak DA release after an initial stimulus is 35% more rapid in α-*Syn*$^{-/-}$ mice, as compared with wt littermates. Stimulation-dependent DA release is depressed in the nucleus accumbens during the establishment of intracranial self-stimulation behavior (Garris et al., 1999), a model of learning and reward. Similarly, activity-dependent regulation of DA release had been suggested to underlie the execution of motor tasks and working memory (Williams and Goldman-Rakic, 1995).

The mechanism of plasticity at DA synapses is poorly understood. In this study, we provide evidence that α-Syn regulates one form of DA plasticity, PSD. We investigated two potential mechanisms of α-Syn action in PSD: modulation of autoreceptor-dependent presynaptic inhibition of neurotransmitter release and regulation of the RRP of synaptic vesicles. In the DA system, autoreceptor-dependent presynaptic inhibition is largely mediated by the DA D2 receptor (through the inactivation of voltage-dependent Ca^{2+} currents; Kennedy et al., 1992). We find that the D2 antagonist sulpiride reduced PSD following train stimulation (train PSD) but did not change the time course of synaptic recovery after a single pulse (single pulse PSD). In contrast, α-Syn deficiency impaired single pulse PSD but not train PSD. These findings argue that α-Syn influences PSD via a DA D2 receptor–independent mechanism. Other inhibitory mechanisms that involve GABA, glutamate, or acetylcholine were not found to play a role in PSD in the DA system (Kennedy et al., 1992). However, we have not excluded an inhibitory role for α-Syn through other yet unidentified presynaptic receptors.

Alternatively, α-Syn may modify PSD by modulating the replenishment of synaptic vesicles at DA synapses. Forms of short-term depression similar to PSD have been described at other CNS synapses (Stevens and Tsujimoto, 1995; Wang and Kaczmarek, 1998). To explain these observations, it has been hypothesized that a limited RRP of synaptic vesicles is present at each synapse and that once this pool is depleted, subsequent synaptic responses are depressed. Thus, restrictions on the size and replenishment rate of the RRP may limit the release capacity of presynaptic terminals, and short-term forms of synaptic depression may represent the time course necessary for regeneration of the RRP (Goda and Südhof, 1997). By analogy, PSD at nigrostriatal synapses may reflect the time necessary to refill a depleted RRP of DA after a prior stimulus. The apparent Ca^{2+} dependence of PSD, combined with the finding that train stimulation accelerated the recovery of DA release at nigrostriatal terminals, provides support for this analogy. Thus, α-Syn may negatively regulate DA release in part by modulating the refilling rate of the RRP. The normal morphology of synaptic terminals and vesicles in the α-*Syn*$^{-/-}$ mice and the physical presence of α-Syn in the direct vicinity of synaptic vesicles (Iwai, 1995) are consistent with such a regulatory rather than structural role. Of note, the two mechanistic models of PSD described above are not mutually exclusive. That is, autoreceptor inhibition may alter the size or refilling rate of the RRP of synaptic vesicles.

A possible molecular mechanism by which α-Syn might regulate vesicular release is suggested by the observation that it is a specific, potent ($K_i = 10$ nM) inhibitor of PLD2 (Jenco et al., 1998). PLD2 catalyzes the hydrolysis of phosphotidylcholine to form PA and DAG (Klein et al., 1995; Jenco et al., 1998), both of which are intracellular mediators that modulate neurotransmitter release. DAG is believed to potentiate neurotransmitter release by increasing the size and recovery rate of the RRP through the activation of protein kinase C, whereas PA has been shown to stimulate vesicle formation (Frohman and Morris, 1996). Thus, α-Syn may negatively regulate DA release in part by inhibiting the formation of DAG and PA by PLD. As α-Syn may interact directly with protein kinase C (Ostrerova et al., 1999) and contains multiple potential phosphorylation sites for this kinase, it may in turn be (positively or negatively) regulated by protein kinase C as part of a feedback pathway. Alternatively, since functional regeneration of RRP requires Ca^{2+}, α-Syn may regulate DA neurotransmission by modulating the levels of intracellular Ca^{2+} or the activity of Ca^{2+}-dependent proteins. It is interesting to note that although α-Syn is prominently expressed in the hippocampus, no deficit in hippocampal LTP was observed. The normal LTP may reflect compensation by β-Syn that is also expressed in this brain region. Alternatively, α-Syn may play a role in PSD but not in other forms of synaptic plasticity.

α-Syn-Deficient Mice Exhibit Decreased Striatal DA Content and Amphetamine Sensitivity

The α-*Syn*$^{-/-}$ mice exhibited significantly reduced levels of total striatal DA, which is primarily stored in synaptic vesicles (Fon et al., 1997). The reduced total striatal DA level in the mutants is not due to a deficit in the density of nigrostriatal DA projections or altered DA reuptake. Instead, consistent with the idea that α-Syn is a negative regulator of RRP, it may reflect an enhanced rate of vesicular trafficking to the RRP and subsequent release. The α-*Syn*$^{-/-}$ mice also display an attenuated locomotor response to amphetamine. This deficit may represent a downstream adaptation (desensitization) to the altered pattern of DA neurotransmission or may be a consequence of the reduced DA content in these animals.

α-Syn Function in Neurodegenerative Disease

α-Syn has been implicated in the pathophysiology of neurodegenerative disorders, including PD and AD, but it remains unclear whether the involvement of this protein in neurodegeneration is at all related to its normal function. A widely held view is that the single amino acid substitutions underlying dominantly inherited PD represent neomorphic mutations and lead to a novel pathological gain of function for this protein. Specifically, it has been hypothesized that mutant α-Syn mediates neuronal degeneration because of a tendency to aggregate and to form toxic inclusion bodies. Abnormal protein aggregates have been described in a number of other neurodegenerative diseases, including tau protein aggregates in frontotemporal dementia (Hong et al., 1998), huntingtin protein aggregates in Huntington's disease (DiFiglia et al., 1997), and prion protein aggregates in Creutzfeld-Jacob disease (Cohen and Prusiner, 1998).

An alternative hypothesis is that human α-Syn mutations might function in a dominant-negative manner and that the inherited disease state might therefore be due to a decrement in the normal function of α-Syn. The fact that α-Syn can dimerize with itself and with other members of this protein family lends support to the dominant-negative hypothesis. Of particular interest in this regard is γ-Syn, which is selectively expressed in DA neurons of the ventral midbrain and may physically interact with α-Syn through a shared putative heterodimerization domain. The mild phenotype that the α-*Syn*$^{-/-}$ mice display argues against the hypothesis that the PD α-*Syn* mutations lead to dominant inactivation of this protein. However, as kindreds that suffer from the human disease remain relatively unaffected for the first three decades of life, it is possible that older α-*Syn* mutant mice would suffer DA neuron loss or that the pathology requires a premorbid period that is longer than the life span of a mouse. Alternatively, dominant-negative forms of α-Syn may lead to a severe phenotype that is not mimicked by α-Syn deficiency through the formation of inactive heterodimers with other members of the Syn protein family, such as γ-Syn. Finally, since one of the pathological mutations in the human α-Syn, A53T, is normally present in wt mice, it is possible that species differences or developmental compensation by the other synuclein family members may be responsible for the mild mouse phenotype.

As α-Syn functions in the regulation of DA release, it represents a potential therapeutic target for PD as well as other movement and psychiatric disorders. Disruption of the synthesis, function, or, possibly, the aggregation of α-Syn would be predicted to increase DA release from the surviving nigral DA neurons and may slow the progression of PD without serious deleterious effects.

Experimental Procedures

Generation of α-*Syn*$^{-/-}$ Mice

Murine α-*Syn* cDNA was amplified from total brain cDNA using α-*Syn*-specific primers (5′-AATACATCTTTAGCCATGGA-3′ and 5′-TCACCCTTGCCCATCTGGTCCTT-3′). A 129SV/j mouse genomic λFixII phage library (Stratagene) was screened with this cDNA to obtain a 14.5 kb NotI genomic fragment encompassing the first three exons of the α-*Syn* gene (encoding amino acids 1–41) and flanking sequences which was subcloned into pBluescriptII (Stratagene). This plasmid was then digested with KpnI to excise a 1.5 kb KpnI genomic fragment. The resulting plasmid was digested with EcoRI and XhoI to excise a 3.2 Kb genomic region encompassing the first three exons of the α-*Syn* gene, which was replaced with a 1.6 Kb MfeI–SalI fragment of plasmid pGT-N39 (New England Biolabs) containing the *PGK-neo* cassette. The resulting targeting vector was linearized with KpnI and electroporated into ES GS cells, which were selected in G418 (400 μg/ml). To identify homologous integration events, BglI-digested genomic DNA isolated from neomycin-resistant clones was hybridized to a KpnI fragment flanking the 3′ terminus of the targeting vector. Three clones with homologous recombination were identified among 200 G418-resistant clones. Chimeric male mice were generated, and these mice were bred to C57/BL6 females to confirm germline transmission. Following heterozygous mating, progeny were genotyped by Southern blotting, as described above, or by PCR analysis with primers specific for exon 2 of α-*Syn* (5′-ATGGATGTGTTCATGAA-AGGACTTTCAA-3′ [designated as "a" in Figure 1]; 5′-TACATAGAGGACTCCCT-CTTTTGTCT-3′ [designated as "b" in Figure 1]) and the neomycin resistance gene (5′-AGGCGATAGAAG-GCGATGCG-3′ [designated as "c" in Figure 1]; 5′-CAAGACCGACCTGTCCGGTG-3′ [designated as "d" in Figure 1]). To confirm the absence of α-*Syn* expression in mutant mice, RT-PCR and Western analyses were performed on brain sections. For RT-PCR analysis, total RNA was isolated from 100 mg cerebral cortex sections using RNAzol (Tel-Test), and cDNA was generated from 5 μg of total RNA. PCR was performed with primers specific for the 5′ terminus (encoding amino acids 1–92; 5′-AGCCATGGATG TGTTCAT-GAAAGG-3′ and 5′-GTGGCAGCAGCTA-TATTCCCAG CT-3′) or the 3′ terminus (encoding amino acids 76–136; 5′-GCA GTCGCTC-AGAAGACAGTGGA-3′ and 5′-AGTCTTG-TAG-CTTCT-CTGAAG-3′). For Western analysis, tissue sections were homogenized in lysis buffer (1% NP-40, 50 mM Tris-Cl [pH 8.0], 150 mM NaCl, 1 mM phenylmethylsulfonyl fluoride, and 10 μM leupeptin), and immunoblot analyses were performed as described using rabbit polyclonal antibodies specific to the carboxyl termini of α-Syn or β-Syn (Chemicon). 129SV/j × C57/BL6 F2 mice that are wt at the α-*Syn* locus were selected for the 129SV/j allele by PCR analysis of a polymorphism within the second intron using the primer pair (5′- ACCAGGAGTTGATGGTCATCTTCAGCT-3′ and 5′-AAGTC-CCA TGAGTACTTGTGGCTCACT-3′).

In Situ Hybridization

Brains from wt and α-*Syn*$^{-/-}$ mice (n = 3 each) were fresh frozen with powdered dry ice, and 16 μm coronal sections were cut on a cryostat. ^{33}P-UTP-labeled RNA probes were synthesized from DNA templates using T7 polymerase. DNA templates were generated by PCR amplification of mouse total brain cDNA with primer pairs specific for α-*Syn* (5′-GGATCCAGCAAAGATACATCTTTAGCC-3′ and 5′-GAATTCTAATACGA-CTCACTATAGGGATTCTTAGGCTT CAG-3′), β-*Syn* (5′-GGATCCCCCCGAAA-CCCAGGCCGCCAG-3′ and 5′-GAATTCTAATACGACTCACTATAGGGCCTGATATTCCTCC TGGGGTG-3′), γ-*Syn* (CAATGAATTCTAATACGACTCACTATAGGG GGACAGAGAACTTGGGCAACCTGC-3′ and 5′-CAATGGATCCAAT-TAACCCTCACTAAAGGGAAGGAGAA-CGTGGTACAAAGTGTCAC-3′),

or *TH* (Hynes et al., 1995). Template identities were confirmed by DNA sequencing. Autoradiographic exposure times were 3 weeks.

Immunohistochemistry

For histological analysis, adult mice were anesthetized with Nembutal and perfused transcardially with 4% paraformaldehyde in 0.1 M phosphate buffer (PB) with or without 0.5% glutaraldehyde. Brains were dissected out and washed in PB, and 50 μm thick sections were obtained in a vibrotome. Sections were incubated in 3% H_2O_2 to quench endogenous peroxidase activity and then blocked for 1 hr in 10% normal goat serum and 0.2% Triton X-100 in PB. Subsequently, sections were incubated overnight with one of the following primary antibodies (dilutions in parentheses): anti-parvalbumin (Swant, Switzerland, 1:8,000), anti-calbindin (Swant, Switzerland, 1:10,000), anti-neuropeptide Y (Incstar, 1:15,000), anti-calretinin (Swant, Switzerland, 1:10,000), anti-somatostatin (Incstar, 1:500), anti-α-Syn (Chemicon, 1:1,000; Santa Cruz C-20, 1:100), anti-β-Syn (Chemicon, 1:1,000), anti-synapsin-I (Synaptic Systems, 1:100), anti-Rab3a (Synaptic Systems, 1:500), or anti-synaptophysin (Boehringer Mannheim, 1:25). Sections were then processed using the ABC peroxidase method (Vector Labs) following the manufacturer's instructions. For DA neuron counts in the SN, serial vibrotome sections through the midbrain were prepared as above and stained with anti-TH antibodies (Pel-Freez, 1:300). Immunoreactive neurons with a visible, well-defined nucleus were counted in alternate sections throughout the SN.

Electron Microscopy

For electron microscopy, adult mice were anesthetized with Nembutal and perfused with 4% paraformaldehyde and 2.5% glutaraldehyde in PB. Brains were dissected out and sectioned coronally at 200 μm with a vibrotome. Sections were postfixed in 2% osmium tetroxide in PB, dehydrated in ascending grades of ethanol, stained in block with 2% uranyl acetate, and then flat embedded in Araldite (Durcupan). Selected areas were sectioned into 1 μm semithin sections and stained with toluidine blue for light microscope analysis. Ultrathin sections containing the striatum (70 nm) were collected in slot grids coated with Formvar film, stained with lead citrate, and observed with a Phillips CM-10 electron microscope. Electron micrographs of random regions of the striatum were generated from at least three different animals per genotype, and synapses were counted. Axon terminals with a visible synaptic contact were drawn and measured using the Visilog software package.

Electrophysiology

Electrical stimulation of striatal slice preparations induces extrasynaptic DA overflow, termed "synaptic overflow," due to the synchronized firing of numerous DA terminals (Garris et al., 1994). Such overflow can be measured at a high temporal and spatial resolution in striatal slice preparations using carbon-fiber electrodes and fast-scan CV (Wightman and Zimmerman, 1990; Kennedy et al., 1992). In CV, a triangular voltage wave is applied to carbon-fiber electrodes (Figure 4A) every 100 ms, and the presence of DA or other catecholamines is deduced from the resultant oxidation current (during the upstroke of the voltage wave) and reduction current (during the downstroke of the voltage wave). DA is positively identified by virtue of the characteristic voltage dependency of its oxidation and reduction reactions. The concentrations of DA are determined by the amplitude of these currents in comparison with a reference standard. Striatal DA release was studied in eight α-*Syn*$^{-/-}$ mice and ten wt littermates, 6–8 weeks old, using CV. Recordings were obtained from the first three coronal slices (300 μm thick), prepared from rostral caudate putamen. Slices were placed in a recording chamber, superfused with artificial cerebrospinal fluid (ACSF) (in mM: NaCl, 124; KCl, 3.7; $NaHCO_3$, 26; $CaCl_2$, 2.4; $MgSO_4$, 1.3; KH_2PO_4, 1.3; and glucose, 10) at 36°C. High-Ca^{2+} ACSF contained 10 mM $CaCl_2$ and 1 mM $MgSO_4$ but was otherwise identical. Carbon-fiber electrodes (5 μm diameter, freshly cut surface) were placed in ventral caudate putamen ~70 μm into the slice. A triangular voltage wave (−400 to +1000 mV at 170 V/s versus Ag/$AgCl_2$) was applied to the electrode every 100 ms using a waveform generator (Wavetek, model 39). Current was recorded with an Axopatch 200B amplifier (Axon Instruments), digitized (Instrunet board, 25 kHz sampling rate), and acquired with a locally written Superscope II program (GWI). DA release was evoked by a bipolar stimulating electrode placed at a 100–150 μm distance from the recording electrode with either single pulse (400 μA, 1 ms) stimulation or a train of 10 pulses at 20 Hz. Background-subtracted cyclic voltammograms served to identify the released substance, which was DA in every case reported. Two-sample Student's t test or two-way ANOVA for repeated measures with subsequent Newman-Keuls test were used for statistical analysis (GB-Stat). Double exponential fitting was performed with Igor software (Wavemetrics). CA1 LTP was elicited by tetanic stimulation (trains of 100 pulses at 100 Hz, repeated four times at 20 s intervals) and recorded in the presence of 10 μM bicuculline at a basal stimulation rate of 0.05 Hz (Castillo et al., 1997; Schlüter et al., 1999). Mossy fiber LTP was induced by tetanic stimulation (trains of 125 pulses at 25 Hz, repeated once after a 20 s interval) and recorded in the presence of 40 μM D-APV (Castillo et al., 1997).

Quantification of DA and DOPAC

Nine α-*Syn*$^{-/-}$ and ten wt mice were analyzed for postmortem tissue content of DA and DOPAC. After cervical dislocation, the brain was removed, immersed in ice-cold PBS for 30 s, placed in a mouse brain coronal matrix on ice (ASI Instruments, Warren, MI), and cut into 1 mm sections. Biopsy punches were used to collect the striatum (from two sections per brain, 13 gauge (13G) anterior and 11G posterior), nucleus accumbens (from one section per brain, 16G), and ventral midbrain (containing the SN and VTA; from two sections per brain, 11G). Brain samples were sonicated in 200 μl of 0.1 M perchloric acid with 0.005% EDTA and 3,4-dihydroxybenzylamine (DHBA) as an internal standard and centrifuged at 23,000–28,000 × g for 20 min at 4°C. The sample pellet was sonicated in 150–1000 μl 0.5 N NaOH, and protein content was determined with the Bio-Rad protein assay (Hercules, CA). DA and DOPAC in the supernatant were quantified by reverse-phase HPLC with electrochemical detection, essentially as described previously (Moore et al., 1996). Samples were injected onto a MetaSil octadecyl silica 3 μm (100 × 4.6 mm) column (MetaChem Technologies, Torrance, CA) perfused with MD-TM mobile phase (ESA, Chelmsford, MA) at 1 ml/min. An ESA Coulochem II electrochemical detector applied −60 mV to electrode 1 and +200 mV to electrode 2 of a coulometric analytical cell (ESA, model 5011). Data were acquired and peak areas calculated with EZChrom Chromatography Data Systems software (Scientific Software, Pleasanton, CA).

Locomotor Activity Assays

Mice (49–83 days old; eight female wt, eleven male wt, four female α-*Syn*$^{-/-}$, and eight male α-*Syn*$^{-/-}$) were tested for spontaneous activity and, 1–6 days later, for amphetamine-induced activity. Total photocell beam breaks per 10 min interval were collected for 2 hr in a 38 × 45 cm Plexiglas arena with an 8 × 8 photocell beam grid (San Diego Instruments). During the first half of the fourth interval, mice received an intraperitoneal injection of 0.9% saline (5 ml/kg body weight) or 4 mg D-amphetamine sulfate/kg body weight (at 0.8 mg/ml 0.9% saline). Two-way ANOVA demonstrated no significant differences between males and females and no interaction between gender and genotype (data not shown), so data from males and females were analyzed together.

Acknowledgments

We thank E. Berry for preparing the manuscript; Allison Bruce and Jim Ligos for assistance with the graphics; Robert Edwards, Robert Malenka, and Sara Jones for useful suggestions; Sharon Erickson, Mabel Chu, and Lucrece Tom for help with genotyping; Linda Loverro and Margaret Kelly for help with animal care; and Almudena G. Yague for assistance with histology. This work was funded in part by the Parkinson's Disease Foundation and the National Institute on Drug Abuse (Y. S. and D. S.).

Received September 13, 1999; revised November 22, 1999.

References

Buchman, V.L., Hunter, H.J., Pinon, L.G.P., Thompson, J., Primalova, E.M., Ninkina, N.N., and Davies, A.M. (1998). Persyn, a member of

the synuclein family, has a distinct pattern of expression in the developing nervous system. J. Neurosci. *18*, 9335–9341.

Castillo, P.E., Janz, R., Südhof, T.C., Tzounopoulos, T., Malenka, R.C., and Nicoll, R.A. (1997). Rab3A is essential for mossy fibre long-term potentiation in the hippocampus. Nature *388*, 590–593.

Clayton, D.F., and George, J.M. (1998). The synucleins: a family of proteins involved in synaptic function, plasticity, neurodegeneration, and disease. Trends Neurosci. *21*, 249–254.

Cohen, F.E., and Prusiner, S.B. (1998). Pathologic conformations of prion proteins. Annu. Rev. Biochem. *67*, 793–819.

Conway, K.A., Harper, J.D., and Lansbury, P.T. (1998). Accelerated in vitro fibril formation by a mutant linked to early-onset Parkinson's disease. Nat. Med. *4*, 1318–1320.

Davidson, W.S., Jonas, A., Clayton, D.F., and George, J.M. (1998). Stabilization of α-synuclein secondary structure upon binding to synthetic membranes. J. Biol. Chem. *273*, 9443–9449.

DiFiglia, M., Sapp, E., Chase, K.O., Davies, S.W., Bates, G.P., Vonsattel, J.P., and Aronin, N. (1997). Aggregation of huntingtin in neuronal intranuclear inclusions and dystrophic neurites in brain. Science *277*, 1990–1993.

Dittman, J.S., and Regehr, W.G. (1998). Calcium dependence and recovery kinetics of presynaptic depression at the climbing fiber to Purkinje cell synapse. J. Neurosci. *18*, 6147–6162.

Fon, E.A., Pothos, E.N., Sun, B.-C., Killeen, N., Sulzer, D., and Edwards, R.H. (1997). Vesicular transport regulates monoamine storage and release but is not essential for amphetamine action. Neuron *19*, 1271–1283.

Frohman, M.A., and Morris, A.J. (1996). Phospholipid signaling: Rho is only ARF the story. Curr. Biol. *6*, 945–947.

Garris, P.A., Ciolkowski, E.L., and Wightman, R.M. (1994). Heterogeneity of evoked dopamine overflow in striatal and striatoamygdaloid regions. Neuroscience *59*, 417–427.

Garris, P.A., Kilpatrick, M., Bunin, M.A., Michael, D., Walker, Q.D., and Wightman, R.M. (1999). Dissociation of dopamine release in the nucleus accumbens from intracranial self-stimulation. Nature *398*, 67–69.

George, J.M., Jin, W.S., Woods, W.S., and Clayton, D.F. (1995). Characterization of a novel protein regulated during the critical period for song learning in the zebra finch. Neuron *15*, 361–372.

Goda, Y., and Südhof, T.C. (1997). Calcium regulation of neurotransmitter release: reliably reliable? Curr. Opin. Cell Biol. *9*, 513–518.

Gomis, A., Burrone, J., and Lagnado, L. (1999). Two actions of calcium regulate the supply of releasable vesicles at the ribbon synapse of retinal bipolar cells. J. Neurosci. *19*, 6309–6317.

Grace, A.A., and Bunney, B.S. (1984). The control of firing pattern in nigral dopamine neurons: burst firing. J. Neurosci. *4*, 2877–2890.

Hong, M., Zhukareva, V., Vogelsberg-Ragaglia, V., Wszolek, Z., Reed, L., Miller, B.I., Geschwind, D.H., Bird, T.D., McKeel, D., Goate, A., et al. (1998). Mutation-specific functional impairments in distinct tau isoforms of hereditary FTDP-17. Science *282*, 1914–1917.

Horger, B.A., Nishimura, M.C., Armanini, M.P., Wang, L.C., Poulsen, K.T., Rosenblad, C., Kirik, D., Moffat, B., Simmons, L., Johnson, E., et al. (1998). Neurturin exerts potent actions on survival and function of midbrain dopaminergic neurons. J. Neurosci. *18*, 4929–4937.

Hynes, M., Poulsen, K., Tessier-Lavigne, M., and Rosenthal, A. (1995). Control of neuronal diversity by the floor plate: contact-mediated induction of midbrain dopaminergic neurons. Cell *80*, 95–101.

Iwai, A., Masliah, E., Yoshimoto, M., Ge, N., Flanagan, L., de Silva, H.A., Kittle, A., and Saito, T. (1995). The precursor protein of non-Aβ component of Alzheimer's disease amyloid is a presynaptic protein of the central nervous system. Neuron *14*, 467–475.

Jakes, R., Spillantini, M.G., and Goedert, M. (1994). Identification of 2 distinct synucleins from human brain. FEBS Lett. *345*, 27–32.

Jenco, J.M., Rawlingson, A., Daniels, B., and Morris, A.J. (1998). Regulation of phospholipase D2: selective inhibition of mammalian phospholipase D isoenzymes by α- and β-synucleins. Biochemistry *37*, 4901–4909.

Jensen, P.H., Sorensen, E.S., Peterson, T.E., Gliemann, J., and Rasumussen, L.K. (1995). Residues in the synuclein consensus motif of α-synuclein fragment, NAC, participate in the transglutaminase-catalysed cross-linking to Alzheimer-disease amyloid βA4 peptide. Biochem. J. *310*, 91–94.

Jensen, P.H., Hojrup, P., Hager, H., Nielsen, M.S., Jacobsen, L., Olesen, O.F., Gliemann, J., and Jakes, R. (1997). Binding of Aβ to α- and β-synucleins: identification of segments in α-synuclein/NAC precursor that bind Aβ and NAC. Biochem. J. *323*, 539–546.

Jones, S.R., Gainetdinov, R.R., Wightman, R.M., and Caron, M.G. (1998). Mechanisms of amphetamine action revealed in mice lacking the dopamine transporter. J. Neurosci. *18*, 1979–1986.

Kennedy, R.J., Jones, S.R., and Wightman, R.M. (1992). Dynamic observations of dopamine autoreceptor effects in rat striatal slices. J. Neurochem. *59*, 449–455.

Klein, J., Chalifa, V., Liscovitch, M., and Loffelholz, K. (1995). Role of phospholipase D activation in nervous system physiology and pathophysiology. J. Neurochem. *65*, 1445–1455.

Krüger, R., Kuhn, W., Müller, T., Woitalla, D., Graeber, M., Kösel, S., Przuntek, H., Epplen, J.T., Schöls, L., and Riess, O. (1998). Ala30Pro mutation in the gene encoding α-synuclein in Parkinson's disease. Nat. Genet. *18*, 106–108.

Lavedan, C. (1998). The synuclein family. Genome Res. *8*, 871–880.

Maroteaux, L., and Scheller, R.H. (1991). The rat brain synucleins; family of proteins transiently associated with neuronal membrane. Brain Res. Mol. Brain Res. *11*, 335–343.

Maroteaux, L., Campanelli, J.T., and Scheller, R.H. (1988). Synuclein: a neuron-specific protein localized to the nucleus and presynaptic nerve terminal. J. Neurosci. *8*, 2804–2815.

Mezey, E., Dehejia, A., Harta, G., Papp, M.I., Polymeropoulos, M.H., and Brownstein, M.J. (1998). α-synuclein in neurodegenerative disorders: murderer or accomplice? Nat. Med. *4*, 755–756.

Moore, M.W., Klein, R.D., Fariñas, I., Sauer, H., Armanini, M., Phillips, H., Reichardt, L.F., Ryan, A.M., Carver-Moore, K., and Rosenthal, A. (1996). Renal and neuronal abnormalities in mice lacking GDNF. Nature *382*, 76–79.

Ostrerova, N., Petrucelli, L., Farrer, M., Mehta, N., Choi, P., Hardy, J., and Wolozin, B. (1999). α-Synuclein shares physical and functional homology with 14-3-3 protein. J. Neurosci. *19*, 5782–5791.

Paik, S.R., Lee, J.-H., Kim, D.-H., Chang, C.-S., and Kim, Y.-S. (1998). Self-oligomerization of NACP, the precursor protein of the non-amyloid β-/A4 (Aβ) component of Alzheimer's disease amyloid, observed in the presence of a C-terminal Aβ fragment (residues 25–35). FEBS Lett. *421*, 73–76.

Polymeropoulos, M.H., Lavedan, C., Leroy, E., Ide, S.E., Dehejia, A., Dutra, A., Pike, B., Root, H., Rubenstein, J., Boyer, R., et al. (1997). Mutations in the α-synuclein gene identified in families with Parkinson's disease. Science *276*, 2045–2047.

Rebec, G.V., Grabner, C.P., Pierce, R.C., and Bardo, M.T. (1997). Transient increases in catecholamine activity in medial prefrontal cortex and nucleus accumbens shell during novelty. Neuroscience *76*, 707–714.

Schlüter, O.M., Schnell, E., Verhage, M., Tzonopoulos, T., Nicoll, R.A., Janz, R., Malenka, R.C., Geppert, M., and Südhof, T.C. (1999). Rabphilin knock-out mice reveal that rabphilin is not required for Rab3 function in regulating neurotransmitter release. J. Neurosci. *19*, 5834–5846.

Seiden, L.S., Sabol, K.E., and Ricaurte, G.A. (1993). Amphetamine: effects on catecholamine systems and behavior. Annu. Rev. Pharmacol. Toxicol. *32*, 639–677.

Spillantini, M.G., Crowther, R.A., Jakes, R., Hasegawa, M., and Goedert, M. (1998). α-Synuclein in filamentous inclusions of Lewy bodies from Parkinson's disease and dementia with Lewy bodies. Proc. Natl. Acad. Sci. USA *95*, 6469–6473.

Starke, K., Gothert, M., and Kilbinger, H. (1989). Modulation of presynaptic release by presynaptic autoreceptors. J. Neurochem. *2*, 449–455.

Stevens, C.F., and Tsujimoto, T. (1995). Estimates for the pool size of releasable quanta at a single central synapse and for the time required to fill the pool. Proc. Natl. Acad. Sci. USA *92*, 846–849.

Stevens, C.F., and Wesseling, J.F. (1998). Activity-dependent modulation of the rat at which synaptic vesicles become available to undergo exocytosis. Neuron *21*, 415–424.

Südhof, T.C. (1995). The synaptic vesicle cycle: a cascade of protein–protein interactions. Nature *375*, 645–653.

Sulzer, D., Chen, T.-K., Lau, Y.Y., Kristensen, H., Rayport, S., and Ewing, A. (1995). Amphetamine redistributes dopamine from synaptic vesicles to the cytosol and promotes reverse transport. J. Neurosci. *15*, 4102–4108.

Tong, G., Malenka, R.C., and Nicoll, R.A. (1996). Long-term potentiation in cultures of single hippocampal granule cells: a presynaptic form of plasticity. Neuron *16*, 1147–1157.

Ueda, K., Fukushima, H., Masliah, E., Xia, Y., Iwai, A., Yoshimoto, M., Otero, D.A.C., Kondo, J., Ihara, Y., and Saitoh, T. (1993). Molecular cloning of cDNA encoding an unrecognized component of amyloid in Alzheimer's disease. Proc. Natl. Acad. Sci. USA *90*, 11282–11286.

Wang, L.-Y., and Kaczmarek, L.K. (1998). High-frequency firing helps replenish the readily releasable pool of synaptic vesicles. Nature *394*, 384–388.

Weinreb, P.H., Zhen, W., Poon, A.W., Conway, K.A., and Lansbury, P.T. (1996). NACP, a protein implicated in Alzheimer's disease and learning, is natively unfolded. Biochemistry *35*, 13709–13715.

Wightman, R.M., and Zimmerman, J.B. (1990). Control of dopamine extracellular concentration in rat striatum by impulse flow and uptake. Brain Res. Brain Res. Rev. *15*, 135–144.

Williams, G.W., and Goldman-Rakic, P.S. (1995). Modulation of memory fields by dopamine D1 receptors in prefrontal cortex. Nature *376*, 572–575.

Wise, R.A. (1996). Addictive drugs and brain stimulation reward. Annu. Rev. Neurosci. *19*, 319–340.